Zeitschrift: Helvetica Physica Acta
Band: 54 (1981)
Heft: 4

Artikel: Direct measurement of the muonium hyperfine frequencies in quartz
Autor: Holzschuh, E. / Kündig, W. / Patterson, B.D.
DOI: https://doi.org/10.5169/seals-115227

Helvetica Physica Acta
Vol. 54, 1981

0018-0238/81/040552-09$1.50+0.20/0
Birkhäuser Verlag, Basel, 1981

Direct measurement of the muonium hyperfine frequencies in quartz

By E. Holzschuh, W. Kündig and B. D. Patterson, Physik-Institut, Universität Zürich, CH-8001 Zürich, Switzerland

(7. XII. 1981)

Abstract. A new method for the measurement of hyperfine frequencies of muonium is described and applied to muonium in quartz. With an apparatus of high time resolution (FWHM = 150 ps), measurements were performed in the temperature range 30–300 K. The results are compared with EPR-studies on atomic H in quartz.

I. Introduction

A positive muon stopped in crystalline quartz may capture an electron and form a muonium atom $Mu = (\mu^+ e^-)$ with high probability (~80%). Quartz is one of the few materials in which the hyperfine transitions of both muonium [1] and atomic hydrogen [2] at an interstitial site have been unambiguously observed. It is therefore of particular interest to have accurate parameters of the Mu hyperfine interaction which can be compared with the EPR results. In Mu the muon and the electron spin may couple parallel or antiparallel (ignoring at present possible small anisotropies in the hyperfine interaction) to form the triplet or the singlet state, respectively. To evaluate the Mu hyperfine interaction one usually measures the splitting of the triplet state as a function of an applied magnetic field (two-frequency method [3]), whereas the higher frequency transitions between the triplet and the singlet states remain unobserved due to limited time resolution. This method is easy to apply but has the disadvantage of a low accuracy.

We report here the observation of the triplet-singlet transition frequencies in quartz in zero external field by the μSR-method [4]. These measurements were made possible by an apparatus with a high resolution timing system. The observed frequencies are the largest μ^+SR-frequencies known to exist without large applied fields. The effects of finite time resolution on high frequency signals are discussed in Section II, and a short description of the apparatus is given. In Section III the pertinent spin Hamiltonians and the expected signals are described. The measurements were performed as a function of temperature in the range 30 to 296 K, and the results are presented in Section IV.

II. Fast timing

In a muon-spin-rotation (μSR) experiment, positive spin-polarized muons are stopped in the sample to be investigated, and the positrons from the muon

decay ($\tau_\mu = 2.2\ \mu s$) are recorded as a function of the time after a muon stop. Since positron emission is most probable in the direction of the muon spin, the counting rate is modulated with the muon precession or oscillation frequencies. If muonium is formed, these frequencies are due to the hyperfine interaction with the bound electron and to the Zeeman energy in an applied field.

For large frequencies the effect of the finite time resolution of the detectors must be considered. The modulation spectrum consists of a sum of terms like

$$f(t) = ae^{-\lambda t}\cos(\omega t), \qquad t > 0, \tag{1}$$

where an exponential damping is assumed. Let $g(t)$ be the normalized resolution function. Then the observed signal is the convolution of g with f

$$f_{\text{obs}}(t) = \int g(t-t')f(t')\,dt'. \tag{2}$$

If g is a 'peaked' function, then for t much larger than the width of g, equation (2) may be written as

$$f_{\text{obs}}(t) \simeq a\ \text{Re}\exp(i\omega - \lambda)t \int g(t')\exp[-(i\omega-\lambda)t']\,dt' \tag{3}$$

$$= ae^{-\lambda t}\ \text{Re}\, Ce^{i\omega t}. \tag{4}$$

The constant $C(|C| \leq 1)$ describes the reduction of the measured signal amplitude and, if g is not an even function, a phase shift. It is important to note, however, that the form and in particular the frequency of the measured signal is independent of the shape of g. To evaluate equation (4), a Gaussian $g(t)$ with $\Delta t =$ FWHM may be assumed. Then C is real and given by (with $\nu = \omega/2\pi$ and $\lambda = 0$):

$$C = a_{\text{obs}}/a = \exp[-(\pi\nu\,\Delta t)^2/(4\ln 2)]. \tag{5}$$

To obtain a reasonable signal, Δt should be less than about $1/(2\nu)$.

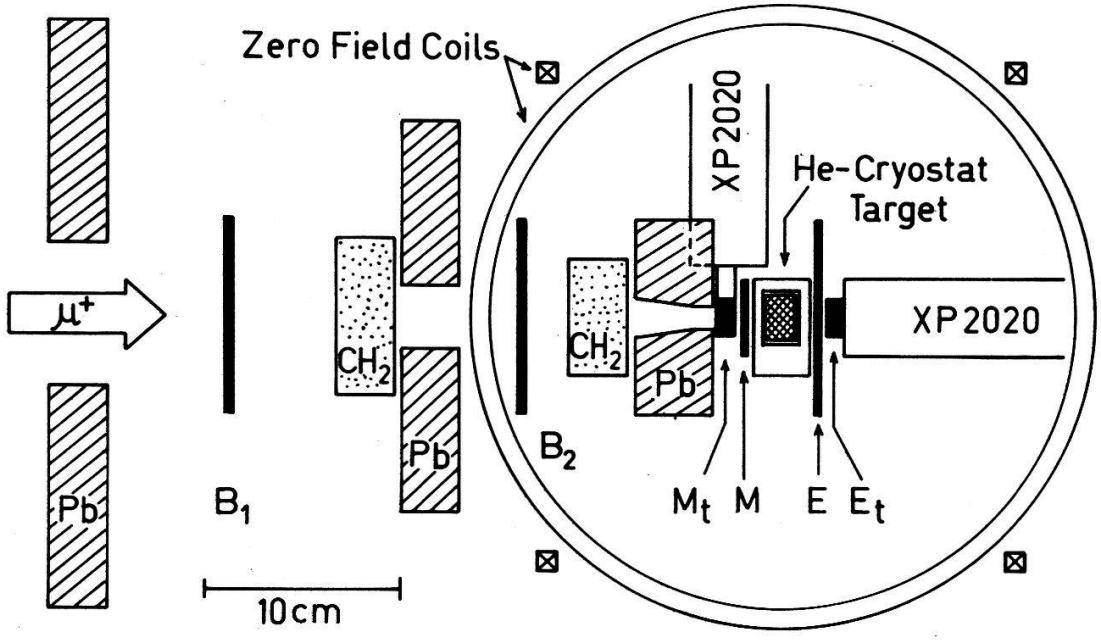

Figure 1
Schematic view of the detector arrangement. Shown are the scintillators (black bars), the lead collimators (Pb), the degrader (CH_2), the cryostat with the target inside and the photomultipliers (XP 2020) of the timing detectors.

The experiments were done with an apparatus similar to other μSR-set-ups, but special care was taken to achieve a high time resolution of the detectors and to maintain a compact geometry around the target. A schematic view of the detector arrangement is shown in Fig. 1. The muon beam is collimated by three lead collimators to a final diameter of 12 mm, degraded by CH_2 and then stopped in the target inside a He-flow cryostat. The plastic scintillators $B1$, $B2$, M and E give the logic signals necessary to distinguish the various possible events such as incoming muons, stopped muons and decay positrons. The timing counters M_t and E_t consist of 10 mm thick NE 111 plastic scintillators attached to XP 2020 photomultiplier tubes. The M_t scintillator has a 20×20 mm^2 area with a 15 mm long light guide, and the E_t scintillator is a disk 20 mm in diameter. The XP 2020 tubes are selected units from a sample of 10. The anode pulses from the timing counters are fed into Ortec 583 differential constant fraction discriminators. The discriminated timing pulses, if coincident with the appropriate logic signals, are fed into the start (M_t) and stop (E_t) inputs of a time-to-amplitude converter (TAC). The TAC time information is digitized by a 8192 channel ADC. In the experiment, the 583-discriminators were adjusted with a ^{60}Co-source, i.e. without beam. Each of the timing signals (M_t, E_t) must pass one fast coincidence, which produces noticeable additional timing error if the coincident logic signals have large timing jitter. Therefore the signals from the $B1$, $B2$, M and E counters are also discriminated by constant fraction discriminators. Figure 2 shows a time resolution spectrum obtained with muons which pass all counters (prompt muon peak), and without degrader or target. The curve plotted is from a fit to a

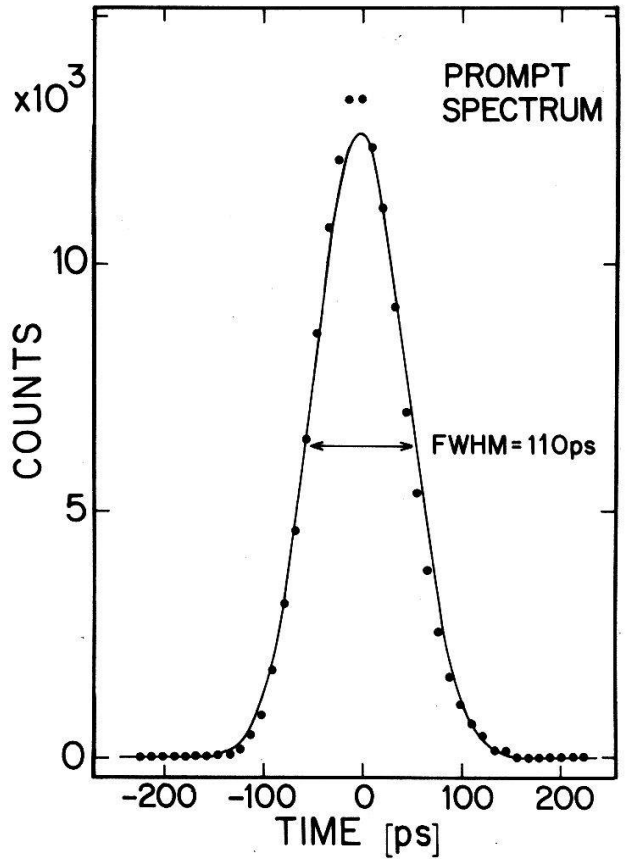

Figure 2
Time resolution spectrum obtained with muons which pass all the detectors without target or degrader. The curve is from a fit to a Gaussian with FWHM = 110 ps.

Gaussian with $\Delta t = \text{FWHM} = 110$ ps. The resolution in the actual experiment was somewhat poorer. This effect will be discussed below.

III. Spin Hamiltonians

Hyperfine interactions (HFI) of two different forms have been found by Brewer et al. [5, 6] for muonium in quartz from observations of intra-triplet state transitions. For temperatures $T \gtrsim 200$ K, the spin Hamiltonian for zero applied field has the form

$$H_s = \nu_0 h \mathbf{I} \cdot \mathbf{S} + \delta h I_z S_z, \tag{6}$$

where $\mathbf{I}$ and $\mathbf{S}$ are spin operators of the muon and the bound electron respectively, and where the symmetry axis z is parallel to the trigonal c-axis of quartz. For $T \lesssim 80$ K a completely anisotropic HFI was found:

$$H_a = A_{11} I_x S_x + A_{22} I_y S_y + A_{33} I_z S_z. \tag{7}$$

An analogous anisotropic state for atomic H has been observed with EPR at $T \lesssim 120$ K in X-irradiated quartz [2, 7]. The directions of the mutually perpendicular principal axes in equation (7) for H are as follows: x is parallel to one of the twofold crystal axes, and the z-axis makes an angle $\alpha = 24.2°$ with the c-axis. Results for muonium are compatible with these directions, but since no definite Mu-values have been published so far, the analysis in this paper will be based on the H-directions.

Equation (6) predicts three and equation (7) six transition frequencies. To assign these frequencies to the experimentally observed signals, the time-dependent muon polarization $P(t)$ in the direction of the positron counter, assumed to be in the direction of the initial polarization, must be calculated. With the normalization $P(0) = 1$ and the notation $\omega = 2\pi\nu$, the result for H_s [equation (6)] is

$$P(t) = \tfrac{1}{2}[\cos^2\theta(1 + \cos\omega_1 t) + \sin^2\theta(\cos\omega_2 t + \cos\omega_3 t)], \tag{8}$$

with

$$\begin{aligned} \nu_1 &= \nu_0 \\ \nu_2 &= \delta/2 \\ \nu_3 &= \nu_0 + \delta/2, \end{aligned} \tag{9}$$

and where θ denotes the angle between the c-axis and the initial polarization.

Denoting the projections of the initial polarization $\mathbf{P}(0)$ along the principal axis j ($j = x, y, z$) in equation (7) by P_j, the result for H_a is

$$P(t) = \tfrac{1}{2} \sum_{j=1}^{3} P_j^2(\cos\omega_j^- t + \cos\omega_j^+ t), \tag{10}$$

with

$$\begin{aligned} \nu_x^{\pm} &= \frac{1}{2h}(A_{22} \pm A_{33}) \\ \nu_y^{\pm} &= \frac{1}{2h}(A_{33} \pm A_{11}) \\ \nu_z^{\pm} &= \frac{1}{2h}(A_{22} \pm A_{11}). \end{aligned} \tag{11}$$

The signs are chosen such that the frequencies are positive for the experimentally determined A-values.

To compare equation (10) with the experimental results, it must be taken into account that there are three equivalent muonium sites associated with the three two-fold crystal axes. Assuming that the c-axis is perpendicular to the initial polarization, as it was in our experiment, the average of the amplitudes over these 3 sites is given by

$$\begin{aligned} \overline{P_x^2} &= \tfrac{1}{2} \\ \overline{P_y^2} &= \tfrac{1}{2}\cos^2\alpha \\ \overline{P_z^2} &= \tfrac{1}{2}\sin^2\alpha. \end{aligned} \tag{12}$$

For the hydrogen value $\alpha = 24.2°$, the amplitude $\overline{P_z^2}$ is much smaller than the other two.

With an external magnetic field B, the Zeeman terms

$$H_z = g_e \mu_B^e \mathbf{B}\cdot\mathbf{S} + g_\mu \mu_B^\mu \mathbf{B}\cdot\mathbf{I} \tag{13}$$

are added to the Hamiltonians, a possible anisotropy in the g-factors having been omitted. Forming the sum $\sum\nu$ and the difference $\Delta\nu$ of the two observable transition frequencies among the triplet states of H_s, the hyperfine frequency ν_0 may be written as

$$\nu_0 = \tfrac{1}{2}[(\textstyle\sum\nu + 2\nu_\mu)^2 - (\Delta\nu + \delta\cos^2\theta)^2] \Big/ \Big[\Delta\nu + \frac{\delta}{2}(3\cos^2\theta - 1)\Big], \tag{14}$$

where $\nu_\mu = |g_\mu|\,\mu_B^\mu B/h$ denotes the Larmor frequency of a free muon, and θ is angle between the symmetry axis z and $\mathbf{B}$. Equation (14) is valid to first order in the parameter $\varepsilon = \frac{1}{4}\delta\sin\theta\cos\theta$ and is exact if $\theta = 0$ or $\delta = 0$. Within the same approximation and under the assumption that the muonic g-factor is not appreciably influenced by the solid host, we obtain in addition

$$g_e = -m_e/m_\mu \cdot g_\mu(\textstyle\sum\nu/\nu_\mu + 1), \tag{15}$$

where $m_\mu/m_e = 206.769$ is the ratio of the muon mass to the electron mass.

IV. Experimental results and discussion

The measurements were performed on a 15 mm thick block of α-quartz with the c-axis perpendicular to the initial muon polarization. The earth field was compensated by three pairs of mutually perpendicular coils (see Fig. 1) to a value smaller than 30 mG over the entire target. The time spectra consisted of 8192 channels with a channel width of about 22.4 ps for the measurements of the fast frequencies. The time scale was calibrated with a quartz calibrator to an absolute accuracy of ±50 ppm. During the measurements the stability of the time scale was ±35 ppm, and the drift of time-zero was smaller than $\pm\frac{1}{2}$ channel. The rate of accumulated events was 150 s^{-1} for a histogram length of 170 ns. Figure 3 shows the Fourier transform of a spectrum at 296 K, obtained in 8 hours of counting

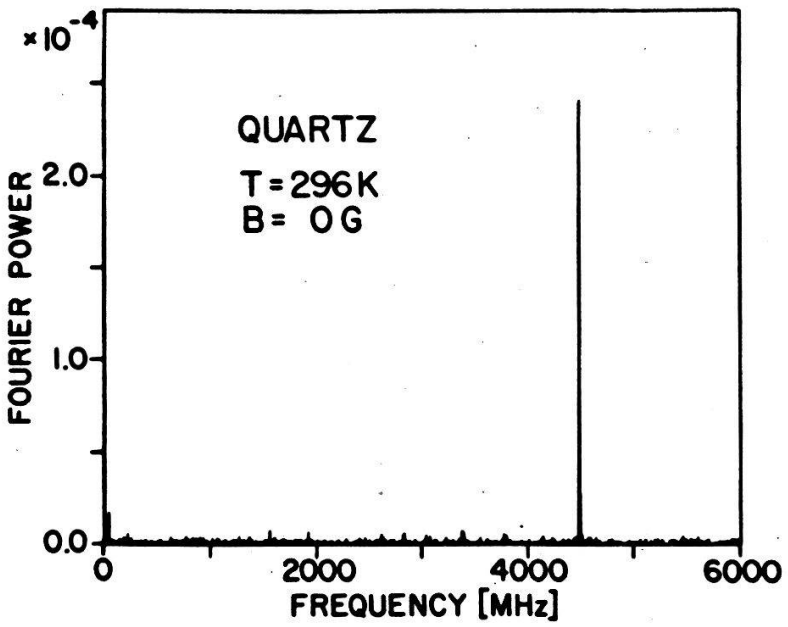

Figure 3
Fourier transform of a spectrum obtained at 296 K with the c-axis perpendicular to the initial muon polarization, showing one transition frequency at 4496 MHz. The small peak at low frequencies is a background signal at the SIN cyclotron frequency (50 MHz). The Fourier power is normalized such that its square root gives the precession amplitude.

time. According to equation (8) the observed frequency is $\nu_3 = \nu_0 + \delta/2$, where $\delta = -0.824(8)$ MHz [8]. The statistical standard deviation of the observed frequency (Fig. 3) is 0.17 MHz. Taking the uncertainty of the time calibration into account we obtain

$$\nu_0(T = 296\text{ K}) = 4496.2 \pm 0.4\text{ MHz}, \tag{16}$$

which is inconsistent with the value published by Brown et al. [9] ($\nu_0 = 4509 \pm 3$ MHz) and measured by the two frequency method.

According to equation (8) the two frequencies ν_2 and ν_3 should theoretically have the same amplitude, and an experimental deviation of their ratio from 1 may be attributed to the effects of a finite time resolution on a_3. The frequencies ν_2 and ν_3 differ by a factor 10^4 and therefore cannot be measured simultaneously. A measurement with an increased histogram length (6.4 μs) gave $\nu_2 = 0.416(4)$ MHz, consistent with Brewer [8]. Then the experimental amplitude ratio $a_3/a_2 = 0.015/0.080$ gives, with equation (5), the effective time resolution $\Delta t = 152 \pm 5$ ps FWHM, which is somewhat larger than the width of the prompt muon peak (Fig. 2). This difference can be attributed to the finite stopping range of the muons (~10 mm FWHM) after they have passed the timing counter M_t with speed $\sim c/2$, giving a minimal stopping time spread of ~70 ps FWHM, and to the smaller energy deposited by the positrons in the scintillator E_t as compared with muons.

A reduction of the amplitude ratio a_3/a_2 may also result from delayed muonium formation. If there is a short-lived precursor state which is transformed into muonium according to a $e^{-t/\tau}$ law, an additional reduction of a_3/a_2 by a factor $1/(1+(\omega_3\tau)^2)^{1/2}$ would result. The analysis of the various contributions to the effective time resolution shows that no such effect is necessary to explain the observed amplitude reduction and gives an upper limit $\tau \lesssim 40$ ps. This excludes

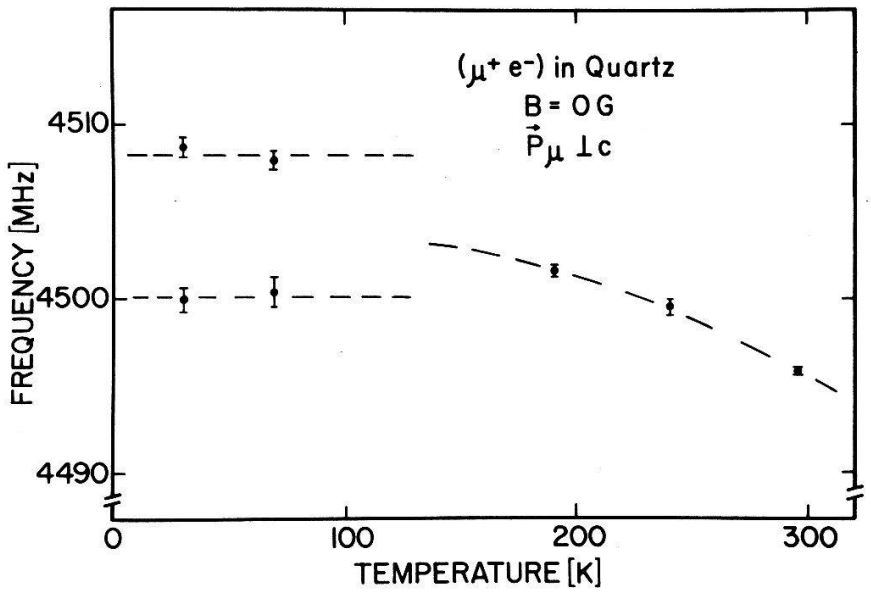

Figure 4
Temperature dependence of the observed fast frequencies. The error bars do not include the systematic errors.

the possibility that muonium formation in α-quartz is related to the diffusion of a thermalized muon to an impurity.

The observed frequencies as a function of temperature are plotted in Fig. 4. There is a noticeable increase of the frequency ν_3 from 296 K to 190 K by 5.9 MHz. At low temperatures, two temperature-independent fast frequencies are observed. In addition there are low frequencies [6] two of which are seen in the Fourier-transform in Fig. 5. Comparing the relative amplitudes of the observed signals with equation (12), a unique assignment of the measured frequencies to the equations (11) can be made if $\alpha \ll 45°$ is assumed. Since the low frequencies

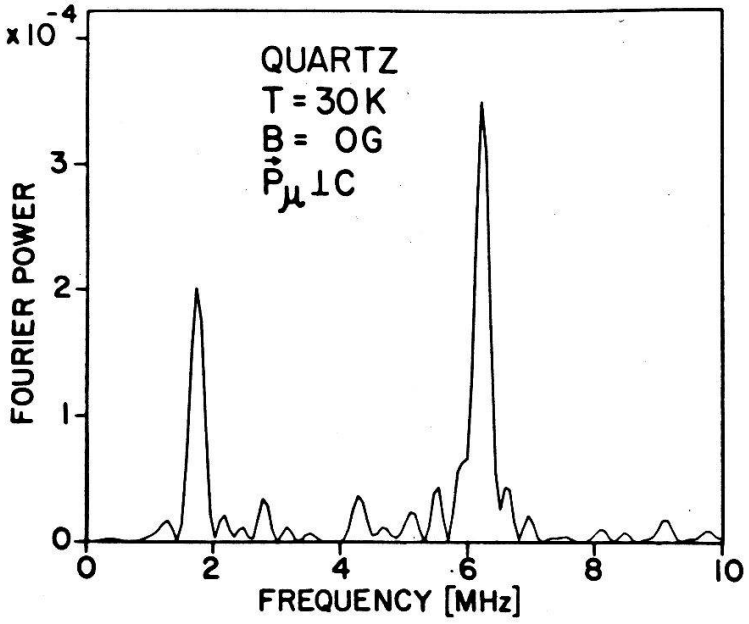

Figure 5
Fourier transform of a spectrum obtained at 30 K with a long time scale, showing the slow transition frequencies.

are measured with more absolute accuracy than the fast ones, it is advantageous to split the HFI A in equation (7) into an isotropic part $A_0 = \frac{1}{3}\,\mathrm{tr}\,(A) = \frac{1}{3}(A_{11}+A_{22}+A_{33})$ and an anisotropic part defined by $\delta_{jj} = A_{jj} - A_0$ and $\mathrm{tr}\,(\delta) = 0$. The result for $T = 30$ K is then:

$$\begin{aligned} A_0/h &= 4505.0 \pm 0.5 \text{ MHz} \\ \delta_{11/h} &= -6.45 \pm 0.02 \text{ MHz} \\ \delta_{22/h} &= +9.44 \pm 0.02 \text{ MHz} \\ \delta_{33/h} &= -2.99 \pm 0.02 \text{ MHz}. \end{aligned} \tag{17}$$

Scaling the hydrogen results by the ratio of the muon-proton magnetic moments, one notes that $\delta_{jj}(H)/\delta_{jj}(\mathrm{Mu}) = 1.45$ within 0.05 including the signs and $A_0(H)/A_0(\mathrm{Mu}) = 1.0128$. A similar relation was noted by Brewer [8] for the observed low frequencies and interpreted as being due to a larger zero-point motion of the Mu compared to H.

Large relaxation effects were observed [8] in the range 100–200 K and interpreted as being due to Mu diffusion which averages the Hamiltonian H_a [equation (7)] to the axial symmetric one [equation (6)]. Extrapolating the weak increase of the high temperature frequency in Fig. 4 to low temperatures suggests that this extrapolated frequency may be an average of the observed fast frequencies. Let us assume that the Mu hops between the 3 equivalent low temperature sites and keeps the bound electron. Then the average of H_a gives H_s [equation (6)] with the symmetry axis z parallel to c and leads to the relations

$$\begin{aligned} h\delta &= \tfrac{3}{2}[\delta_{33} + (\delta_{11} - \delta_{33}) \sin^2 \alpha] \\ h\nu_0 &= A_0 - \tfrac{1}{3}h\delta. \end{aligned} \tag{18}$$

With the values in equation (17) and with $\alpha = 24.2°$, one obtains $\delta = -5.4$ MHz which has the right sign, but the absolute value is far too large. We may conclude from this that the HFI observed at high temperatures is not merely an average over sites, but that in addition the effective HFI becomes weaker with increasing temperature. This is also suggested by the decrease of the observed frequency in Fig. 4.

The discrepancy of the directly measured frequency ν_0 [equation (16)] with the value obtained by the two frequency method [9] at room temperature made it appear necessary to make measurements with an external field. Such differences may result if the Hamiltonian H_s would be not correct. Measurements with a standard μSR-set-up were performed at room temperature with the c-axis parallel to the external field up to 450 Gauss, and ν_0 was calculated from equation (14). The average value of these measurements is $\nu_0 = 4496.7 \pm 1.4$ MHz, fully consistent with the result of the direct measurement. In addition, the electron g-factor was obtained [equation (15)], $g_e = 2.0034 \pm 0.0035$, consistent with the vacuum value.

V. Conclusions

A new method for measurements of muonium hyperfine parameters has been described and its usefulness demonstrated with quartz as an example. The

observed frequencies are the largest μ^+SR-frequencies known to exist without large applied fields. At present the statistical accuracy is about a factor of 5–10 better than obtainable by the two frequency method within the same counting time. This could be further improved if a high resolution clock with a time scale comparable to the muon life time could be used. Such a clock should be possible with present day technology.

The observation of very high frequencies gives stringent limits for the muonium formation time and excludes all models which assume muonium formation by thermal diffusion to defects.

The high accuracy allowed the observation of a small temperature dependence of the HFI in quartz. Such effects can be caused by phonon interaction or by lattice expansion. To find the correct interpretation, measurements with high pressure are necessary, which can also be done by the direct method.

REFERENCES

[1] G. G. MYASISHCHEVA, Y. V. OBUKHOV, V. S. ROGANOV and V. G. FIRSOV, Sov. Phys. JETP *26*, 298 (1968).
[2] B. D. PERLSON and J. A. WEIL, J. Magn. Reson. *15*, 594 (1974).
[3] I. I. GUREVICH, I. G. IVANTER, E. A. MELESHKO, B. A. NIKOL'SKII, V. S. ROGANOV, V. I. SELIVANOV, V. P. SMILGA, B. V. SOKOLOV and V. D. SHESTAKOV, Sov. Phys. JETP *33*, 253 (1971).
[4] J. H. BREWER and K. M. CROWE, Ann. Rev. Nucl. Part. Sci. *28*, 239 (1978).
[5] J. H. BREWER, D. S. BEDER and D. P. SPENCER, Phys. Rev. Let. *42*, 808 (1979).
[6] J. H. BREWER, D. P. SPENCER, D. G. FLEMING and J. A. R. COOPE, *Hyperfine Interactions 8*, 405 (1981).
[7] J. A. WEIL, *Hyperfine Interactions 8*, 371 (1981).
[8] J. H. BREWER, *Hyperfine Interactions 8*, 375 (1981).
[9] J. A. BROWN, S. A. DODDS, T. L. ESTLE, R. H. HEFFNER, M. LEON and D. A. VANDERWATER, Solid State Com. *33*, 613 (1980).